Organic Electronics 35 (2016) 142–150

Contents lists available at ScienceDirect

Organic Electronics

journal homepage: www.elsevier.com/locate/orgel

Simple molecular structure design of iridium(III) complexes: Achieving highly efficient non-doped devices with low efficiency roll-off

Li-Li Wen [a], Jing Yu [b], Hai-Zhu Sun [a], Guo-Gang Shan [a, *], Kai-Yue Zhao [a], Wen-Fa Xie [b, **], Zhong-Min Su [a, ***]

[a] Institute of Functional Material Chemistry, Faculty of Chemistry, Northeast Normal University, Changchun 130024, PR China
[b] State Key Laboratory on Integrated Optoelectronics, College of Electronic Science and Engineering, Jilin University, Changchun, Jilin 130012, PR China

ARTICLE INFO

Article history:
Received 19 January 2016
Received in revised form
29 March 2016
Accepted 5 May 2016

Keywords:
Iridium(III) complex
Simple molecular structure
Non-doped device
Improved efficiency
Low roll-off
DFT

ABSTRACT

To construct efficient emitters suitable for non-doped devices and deeply understand the relationship between structures and performances, we designed and synthesized two heteroleptic iridium(III) complexes based on 1,2-diphenyl-1*H*-benzoimidazole (PBI) ligands whose substituents are varied simply from methyl (complex **2**) to *tert*-butyl groups (complex **3**). The parent complex **1** with non-substituent on PBI ligand has also been presented for a better comparison. Their photophysical, electrochemical and electroluminescent (EL) performances are investigated systematically. Despite their structural modification, all complexes exhibit almost identical emission and excited-state characters, which are rationalized by the quantum-chemical calculations. However, the obvious differences on device performances are found. Non-doped device employing **3** as emitting layer displays the highest EL performance with maximum current efficiency ($\eta_{c,\ max}$) of 18.6 cd A^{-1} and power efficiency ($\eta_{p,\ max}$) of 16.2 lm W^{-1} accompanied by low efficiency roll-off values, which is much higher than those of complexes **1** and **2**. The obtained results herein suggest that introduction of the simple substituent into PBI ligand is an effective and feasible approach to develop highly efficient non-doped phosphors.

1. Introduction

Organic light emitting diodes (OLEDs) have attracted tremendous attention in both academic and industrial laboratories since the first report from Tang and VanSlyke in solid-state lighting sources and flat-panel displays [1–3]. In the past several decades, intense and growing efforts have been devoted to the development of new OLEDs materials to satisfy market requirements [4–7]. Compared with fluorescent emitters, the phosphorescent ones can harvest both singlet and triplet excitons to achieve a theoretical internal quantum efficiency of 100% [8–20]. Phosphorescent emitters are generally complexes composed of second- and third-row transition metals, such as Pt(II) [21–29], Ru(II) [30], Os(II) [31,32] and Ir(III)-based [33–35] complexes. Among them, iridium(III) complexes are emerged as promising materials owing to their high quantum efficiency, high thermal stability, relatively short excited state lifetime as well as wide color tunability [36]. To avoid self-quenching effect caused by strong intermolecular interaction, phosphorescent OLEDs (PhOLEDs) are usually fabricated using host-guest emitting system with dispersing of the iridium(III) complexes in a proper host matrix [37–50]. However, the concentration of emitting materials blended in host matrix is usually lower than 10 wt%, which is hard to precisely control and prevents OLEDs from being reproduced for mass production processes. Moreover, the phase segregation is inevitable, further deteriorating the device stability and lifetime [51].

Non-doped devices can resolve the aforementioned issues and simplify the process of device fabrication, holding great potential for mass production. Whereas, the external quantum efficiencies of non-doped PhOLEDs remain far below those of reported state-of-

* Corresponding author.
** Corresponding author.
*** Corresponding author.
E-mail addresses: shangg187@nenu.edu.cn (G.-G. Shan), xiewf@jlu.edu.cn (W.-F. Xie), zmsu@nenu.edu.cn (Z.-M. Su).

http://dx.doi.org/10.1016/j.orgel.2016.05.002
1566-1199/

the-art doped ones, which are usually caused by aggregation-caused quenching effect in the films [52,53]. A key challenge in developing non-doped devices is to employ phosphorescent emitters with low triplet quenching in the neat films. The introduction of bulky dendritic groups to iridium(III) complexes is an efficient strategy to reduce the intermolecular interaction and enhance the phosphorescent emission quantum efficiency [54–56]. For example, iridium(III) dendrimers with carbazole-based and diphenylamine-based dendrons have been synthesized to successfully reduce the strong intermolecular interactions [57–59]. However, it is a complicated process of introducing so large groups into the ligands. Thus, iridium(III) complexes that combine high efficiency with the simple synthesis are highly desirable. Previous works indicated that 1,2-diphenyl-1*H*-benzoimidazole (PBI) is an excellent building block in the construction of iridium(III) complexes suitable for non-doped phosphors [60,61]. However, there is still much room for improvement in electroluminescent (EL) efficiencies, the simple and feasible design strategy to improve the device efficiency is needed to explore.

To further develop the appropriate iridium(III) phosphors for efficient non-doped devices and investigate the structure-property relationship, in this work, we designed and synthesized three green heteroleptic iridium(III) complexes containing an increasingly bulky substituent on the PBI ligand (Scheme 1). Meanwhile, the 2-(5-(trifluoromethyl)-2*H*-1,2,4-triazol-3-yl)pyridine (Htfmptz) is selected as the ancillary ligand. The 1,2,4-triazole ring with the electron-rich nature can improve the electron-transporting capability. The triazole and second pyridyl fragment display the strong σ-donor and π-accepting property, respectively, enhancing the chelating interaction. Moreover, Htfmptz holds the stronger electronegativity with the $-CF_3$ group introduced into the 1,2,4-triazole ring, which can led to a larger energy gap, consequently, blue-shift emission spectra [62,63]. The photophysical, electrochemical and EL properties of complexes **1**–**3** are investigated systematically. In comparison to complexes **1** and **2**, the efficiencies of complex **3** are significantly improved in both doped and non-doped OLEDs. Significantly, promising EL performance with a maximum current efficiency ($\eta_{c,\ max}$) of 18.6 cd A^{-1} and a maximum power efficiency ($\eta_{p,\ max}$) of 16.2 lm W^{-1} are successfully achieved in the non-doped device based on **3**. Moreover, this non-doped device displays low efficiency roll-off at high brightness.

2. Experimental

2.1. General

Ultraviolet–visible (UV–vis) absorption spectra were recorded on Cary 500 UV–vis–NIR spectrophotometer and emission spectra were measured using FL-4600 FL spectrophotometer. The neat films of **1**–**3** were prepared through spin-coating a solution of them in CH_2Cl_2 (20 mg mL^{-1}) on precleaned glass substrates at 2000 rpm. The photoluminescence quantum yields (PLQYs) in neat films were measured in an integrating sphere. Cyclic voltammetry (CV) were carried out on a BAS 100 W instrument containing 0.1 M tetra-butylammonium hexa-fluorophosphate in CH_2Cl_2 as a supporting electrolyte with a scan rate of 100 mV s^{-1}. A glassy carbon working electrode, a platinum auxiliary electrode, and an aqueous saturated calomel reference electrode were used and the potentials were referenced against ferrocene. The ^{1}H NMR data were recorded on Bruker Avance 500 MHz spectrometer with tetramethylsilane as internal standard.

2.2. Synthesis

Ancillary ligand 2-(5-(trifluoromethyl)-2*H*-1,2,4-triazol-3-yl) pyridine (Htfmptz) was synthesized according to the previously reported method [64].

2.2.1. Synthesis of cyclometalated ligands

2.2.1.1. Synthesis of PBI. To a solution of *N*-phenyl-*o*-phenylenediamine (9.21 g, 50.00 mmol) in *N*,*N*-dimethylacetamide (20 mL), benzoyl chloride (7.00 g, 50.00 mmol) was added slowly under nitrogen atmosphere and the mixture was stirred for 1 h at room temperature. After addition of water, the precipitated solid was filtered off and washed with water and methanol. The solid was recrystallized from a *N*,*N*-dimethylacetamide/water mixture and then added into acetic acid (25 mL) under reflux. The solvent was evaporated and purified by column chromatography on silica gel. Synthesis of MePBI and tBuPBI were similar to PBI. ^{1}H NMR (500 MHz, $CDCl_3$, δ [ppm]): 7.90 (d, J = 8.5 Hz, 1H), 7.57 (d, J = 7.0 Hz, 2H), 7.52–7.45 (m, 3H), 7.37–7.25 (m, 8H).

2.2.1.2. Synthesis of MePBI. ^{1}H NMR (500 MHz, $CDCl_3$, δ [ppm]): 7.89 (d, J = 8.0 Hz, 1H), 7.52–7.45 (m, 5H), 7.35–7.31 (m, 3H), 7.27–7.23 (m, 2H), 7.11 (d, J = 8.0 Hz, 2H), 2.34 (s, 3H).

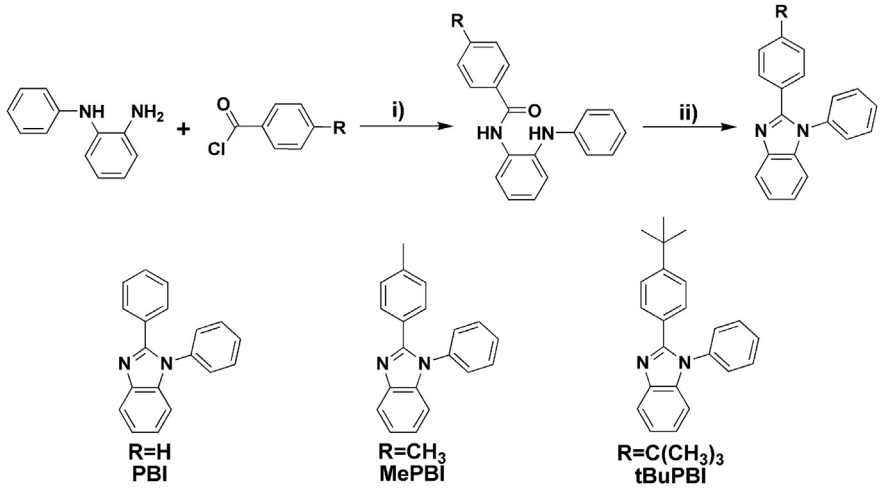

Scheme 1. Syntheses of cyclometalated ligands PBI, MePBI, and tBuPBI. i) DMA, stir, 1 h ii) HAc, reflux.

2.2.1.3. Synthesis of tBuPBI. ^{1}H NMR (500 MHz, $CDCl_3$, δ [ppm]): 7.88 (d, J = 8.0 Hz, 1H), 7.53–7.48 (m, 5H), 7.35–7.30 (m, 5H), 7.26–7.21 (m, 2H), 2.29 (s, 9H).

*2.2.2. Synthesis of complexes **1**–**3***

Synthetic route of complexes **1**–**3** is shown in Scheme 2. All complexes were fully characterized by ^{1}H NMR spectrometry, MALDI-TOF mass spectrometry, high resolution mass spectra (HRMS) (see the Experimental Section). In addition, complex **2** was characterized by single-crystal X-ray diffraction, the structure and data are shown in the Fig. S1 and Table S1 (ESI).

*2.2.2.1. Synthesis of complex **1**.* PBI (0.59 g, 2.20 mmol) and $IrCl_3 \cdot 3H_2O$ (0.35 g, 1.00 mmol) were mixed in 2-ethoxyethanol/water (3:1, 20 mL). The reaction mixture was stirred and heated to reflux for 24 h under nitrogen atmosphere. After cooling to room temperature, the product was filtered, washed with water, ethanol and diethyl ether. The product was isolated as a yellow powder. To a suspension of dimer $[Ir(pbi)_2(\mu\text{-}Cl)]_2$ (0.37 g, 0.24 mmol) in dichloromethane/ethanol (3:1, 60 mL) was added Htfmptz (0.13 g, 0.60 mmol). The reaction mixture was stirred and heated to reflux for 18 h under nitrogen atmosphere, and the product was extracted by dichloromethane. The organic phase was washed with water, dried over by anhydrous Na_2SO_4 and the solvent was evaporated. The product was then purified by column chromatography on silica gel. The pure product was isolated as a powder. ^{1}H NMR (500 MHz, DMSO-d_6, δ [ppm]): 8.42 (d, J = 8.0 Hz, 1H), 8.19–8.16 (m, 1H), 7.92 (d, J = 5.5 Hz, 1H), 7.82–7.78 (m, 7H), 7.74–7.72 (m, 1H), 7.66–7.64 (m, 1H), 7.59–7.56 (m, 1H), 7.52 (d, J = 7.5 Hz, 1H), 7.27–7.21 (m, 2H), 7.11–7.07 (m, 3H), 7.00–6.98 (m, 1H), 6.79–6.76 (m, 1H), 6.69 (t, J = 6.5 Hz, 1H), 6.67–6.64 (m, 1H), 6.57–6.51 (m, 2H), 6.47–6.43 (m, 2H), 5.99 (d, J = 8.5 Hz, 1H), 6.32 (d, J = 7.5 Hz, 1H), 5.71 (d, J = 3.0 Hz, 1H). MS (MALDI-TOF): m/z 944.2. HRMS m/z: $[M]^+$ calcd for $C_{46}H_{30}F_3IrN_8$, 944.2175; found: 944.2149.

*2.2.2.2. Synthesis of complex **2**.* Synthesis of complex **2** was similar to **1**. ^{1}H NMR (500 MHz, DMSO-d_6, δ [ppm]): 8.41 (d, J = 7.5 Hz, 1H), 8.16 (t, J = 8.0 Hz, 1H), 7.95 (d, J = 5.0 Hz, 1H), 7.81–7.78 (m, 7H), 7.64 (d, J = 7.0 Hz, 1H), 7.58 (t, J = 6.5 Hz, 1H), 7.52 (d, J = 1.5 Hz, 2H), 7.24–7.18 (m, 2H), 7.07 (t, J = 7.0 Hz, 3H), 6.97 (t, J = 8.0 Hz, 1H), 6.51 (d, J = 8.0 Hz, 1H), 6.42–6.31 (m, 2H), 6.32 (d, J = 7.0 Hz, 1H), 6.23 (s, 1H), 6.08 (s, 1H), 5.92 (d, J = 9.0 Hz, 1H), 5.68 (d, J = 8.0 Hz, 1H), 1.10 (s, 3H), 1.94 (d, J = 9.5 Hz, 1H). MS (MALDI-TOF): m/z 972.2. HRMS m/z: $[M]^+$ calcd for $C_{48}H_{34}F_3IrN_8$, 972.2488; found: 972.2465.

*2.2.2.3. Synthesis of complex **3**.* Synthesis of complex **3** was similar to **1**. ^{1}H NMR (500 MHz, DMSO-d_6, δ [ppm]): 8.45 (d, J = 7.5 Hz, 1H), 8.16 (t, J = 8.5 Hz, 1H), 7.87 (d, J = 8.5 Hz, 1H), 7.85–7.75 (m, 7H), 7.70 (d, J = 8.5 Hz, 1H), 7.55 (t, J = 6.0 Hz, 1H), 7.31–7.30 (m, 1H), 7.28–7.22 (m, 3H), 7.15–7.10 (m, 3H), 7.03 (t, J = 8.5 Hz, 1H), 6.75–6.73 (m, 1H), 6.61–6.59 (m, 1H), 6.39 (d, J = 8.0 Hz, 1H), 6.34 (d, J = 1.5 Hz, 1H), 6.31 (d, J = 8.5 Hz, 1H), 6.28 (s, 1H), 6.15 (d, J = 8.5 Hz, 1H), 5.79 (d, J = 8.5 Hz, 1H), 0.86 (d, J = 6.0 Hz, 9H), 0.83 (s, 9H). MS (MALDI-TOF): m/z 1056.3. HRMS m/z: $[M]^+$ calcd for $C_{54}H_{46}F_3IrN_8$, 1056.3427; found: 1056.3404.

2.3. Theoretical calculations

All computations and the geometry optimization were performed with the Gaussian 09 software package. The geometrical structures of ground and lowest triplet states for **1**–**3** were fully optimized with C1 symmetry constrains by using the restricted closed-shell and spin-unrestricted open-shell B3LYP methods [65], respectively. The "Double-ζ" quality basis sets for C, H, N atoms was 6-31G*, while the LANL2DZ was employed for Ir atom. The effective core potential replaced the inner core electrons of iridium leaving the outer core $(5s)^2(5p)^6$ electrons and the $(5d)^6$ valence electrons of iridium (III). The expectation values calculated for S^2 were small than 2.05 in spin-unrestricted calculations. To investigate the excited-state electronic properties of studied complexes, Tamm-Dancoff Approximation (TDA) in the time-dependent density functional theory (TD-DFT) calculations were performed in the

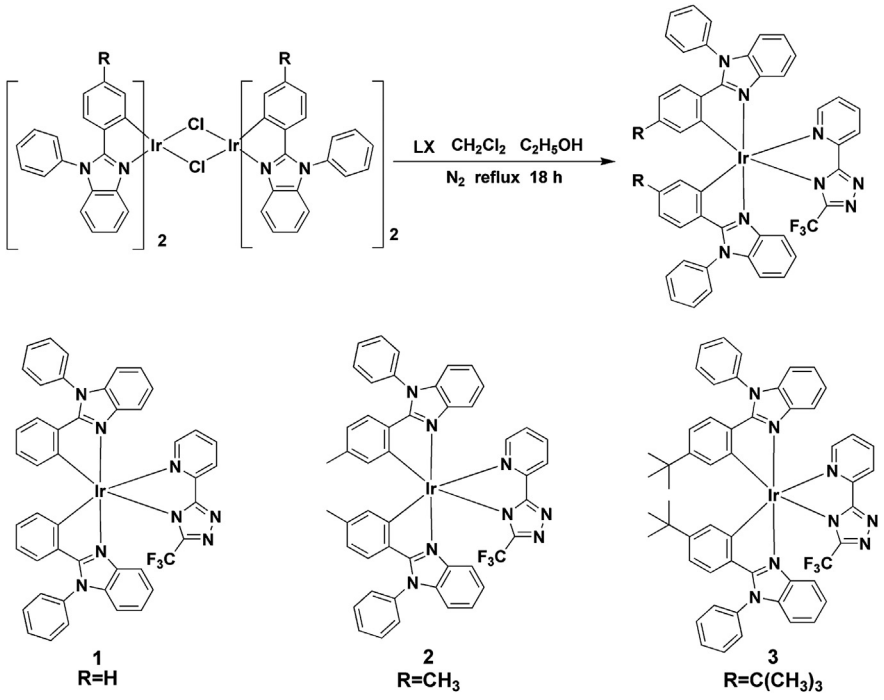

Scheme 2. Synthetic route of complexes **1**–**3**.

presence of the solvent (dichloromethane) at the optimized T_1 geometries. Dichloromethane was chosen as the solvent because the spectra studied in this work were recorded in it, which could act as the limiting case compared with the gas-phase.

2.4. OLEDs fabrication and measurements

OLEDs were fabricated onto cleaned indium-tin-oxide (ITO) glass substrates with the sheet resistance of 20 Ω per square. The ITO substrates were subjected to a routine cleaning process with rinsing in Decon 90, deionized water, drying in an oven and finally treating in a UV-ozone chamber. Organic layers and cathode were sequentially deposited on the glass substrates without breaking vacuum (~5.0×10^{-4} Pa), a shadow mask was used to define cathode and make four 10 mm^2 device each substrates. The thickness of the organic layers and metal were monitored in-situ with quartz oscillator. Luminance-current-voltage characteristics for the unpackaged devices were measured simultaneously with a programmable Keithley 2400 source meter and a Minolta luminance meter LS-110. The spectra of the devices were measured with an Ocean Optics Maya 2000-PRO spectrometer. All the measurements were carried out at room temperature in air.

2.5. X-ray crystallography

Single crystal of **2** was grown from slow vapor diffusion of dichloromethane. The single-crystal X-ray diffraction data for complex **2** were collected on a Bruker Apex CCD II area-detector diffractometer with graphite-monochromated Mo Kα radiation ($\lambda = 0.71069$ Å) at 293(2) K. Absorption correction was applied by using multi-scan technique. The structure of **2** was solved by Direct Method of SHELXS-97 and refined by full-matrix least-square techniques using the SHELXL-97 program [66]. Metal atom in **2** was located from the E-maps and non-hydrogen atoms were located in successive difference Fourier syntheses and refined with anisotropic thermal parameters on F^2. Hydrogen atoms were calculated in ideal geometries. Further details of the crystal structure determination have been deposited to the Cambridge Crystallographic Data Centre as supplementary publication. CCDC 1469412 contains the supplementary crystallographic data for this paper.

3. Results and discussion

3.1. Photophysical properties

The absorption and photoluminescence (PL) spectra of complexes **1**–**3** were recorded in dichloromethane solutions at room temperature and the photophysical data are collected in Table 1. Complexes **1**–**3** display strong absorption bands at 310 nm, which are mainly attributed to spin-allowed ligand-centered $^1\pi$-π^* transition localized on cyclometalated and ancillary ligands. The weak bands in the lower energy region longer than 325 nm can be assigned to MLCT (metal to ligand charge-transfer), LLCT (ligand to ligand charge-transfer) and $^3\pi$-π^* (^{3}LC) transitions of complexes **1**–**3** [67]. Obviously, all complexes exhibit the identical absorption spectra except for absorption intensity, demonstrating that additional substituents have little influence on the electronic and vibrational structures of the ground-states and the first excited-states [68].

As shown in the Fig. 1, complexes **1**–**3** exhibit similar shape with green emission at room temperature in CH_2Cl_2 solution, despite the different size substituents attached to the PBI ligand. The PL spectra have vibronically structured features with the main peak at 496 nm and a shoulder at 524 nm, respectively, which is probably due to the ^{3}LC character of the excited state [69]. The excited-state lifetimes (τ) of complexes **1**–**3** in degassed CH_2Cl_2 are measured as 0.35, 0.50, and 0.69 μs at ambient temperature, respectively, confirming the phosphorescent feature of these iridium(III) complexes. As shown in Fig. S2 (ESI), complexes **1**–**3** emit strong phosphorescence at 487 nm in dichloromethane at 77 K, showing more structured emission spectra. In addition, the PL spectra in low temperature exhibit blue-shifts (9 nm) compared with those at room temperature, which is explained by the rigidochromic effect caused by their intrinsic ^{3}MLCT excited characters [70]. Thereby, we concluded that the observed emission of complexes **1**–**3** should originate not only from ^{3}MLCT excited state but also from ^{3}LC states.

Furthermore, these complexes in spin-coated films also show the strong emission (Fig. S3 in the ESI) with smaller bathochromic shift compared to those in solution, probably resulting from their weak self-aggregation in the solid [69]. Complex **2** show lower PLQY in neat film, possibly due to the weak steric hindrance of methyl unit. It is speculated that the device performance might be similar for both complexes **1** and **2**. However, the highest PLQY of the neat films was obtained for complex **3**, measured to be 15.3%, which is much higher than that of complexes **1** and **2**. The results demonstrate that intermolecular interaction between the molecules in the neat film of **3** is decreased by introducing large substituent, resulting in the desired increase in PLQY [56,71].

To further investigate the nature of the experimentally observed emission behaviors, TD-DFT calculations were conducted to determine the emitting excited-state characteristics of complexes **1**–**3**. The highest-occupied and the lowest-unoccupied molecular orbitals (HOMO and LUMO, respectively) distributions of all complexes are displayed in Fig. 2. The excited energy states, orbital compositions and their assignments of complexes **1**–**3** are listed in Table 2. It is clearly seen that, the frontier orbitals distributions of complexes **1**–**3** are nearly identical, in which the HOMO is primarily distributed on the benzoimidazole group of the cyclometalated ligand and the iridium ion, whereas the LUMO is mainly located on the benzoimidazole moiety. There is no distribution on

Table 1
Photophysical properties of complexes **1**–**3**.

Complex	$\lambda_{PL,max}$[a,b,c] (nm)	τ[a] (μs)	E_{ox}[d] (V)	E_g[e] (eV)	HOMO[f] (eV)	LUMO[g] (eV)	Φ_p (%)
1	496, 487, 503	0.35	1.14	2.69	−5.16	−2.47	12.4
2	496, 487, 520	0.50	1.10	2.70	−5.12	−2.42	8.4
3	494, 487, 504	0.69	1.07	2.73	−5.09	−2.36	15.3

[a] Measured in CH_2Cl_2 (10^{-5} M) at room temperature.
[b] Measured in CH_2Cl_2 (10^{-5} M) at 77 K.
[c] Measured in neat film.
[d] Measured by CV with ferrocene as the standard.
[e] Estimated referring to the overlap between the absorption and emission spectra in CH_2Cl_2.
[f] Calculated from onset oxidation potential.
[g] Deduced from HOMO and E_g.

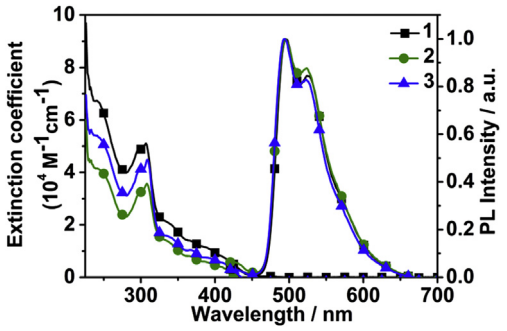

Fig. 1. Absorption and emission spectra of complexes **1**–**3** in CH_2Cl_2 solutions at room temperature.

the substituent, demonstrating that the added bulky moieties do not significantly affect the excited states, which coincide well with the experimental emission spectra. The theoretical results demonstrated that the T_1 states of these complexes mainly contributed by HOMO → LUMO with a configuration interaction coefficient larger than 0.86, composed of the mixed ^{3}MLCT and ^{3}LC character [72].

3.2. Electrochemical properties

The electrochemical properties of the complexes **1**–**3** were investigated by cyclic voltammetry, and the relevant electrochemical date are listed in Table 1. The complexes **1**, **2**, and **3** possess onset oxidation at 1.14, 1.10, and 1.07 eV, respectively, which are assigned to the oxidation of iridium metal-centered Ir^{III}/Ir^{IV} [73]. The HOMO energy levels of complexes **1**–**3** were thus determined from the onset of the oxidation potentials with regard to the energy level of ferrocene, −5.16 eV for **1**, −5.12 eV for **2**, and −5.09 eV for **3**. The LUMO levels were evaluated from the HOMO energy levels and energy gaps determined by the onset of absorption, with 2.47 eV for **1**, 2.42 eV for **2**, and 2.36 eV for **3**. These data are essential to fabricate the green EL devices based on complexes **1**–**3**.

3.3. Eletroluminance properties

3.3.1. Non-doped green eletrophosphorecense

To evaluate the EL performance of all complexes, three phosphorescent non-doped devices have been fabricated based on complexes **1**–**3** by vacuum evaporation method, namely **N1**, **N2**, and **N3**, respectively. Devices with the same configuration of ITO/TAPC (35 nm)/TCTA (5 nm)/Ir complexes **1**–**3** (20 nm)/TmPyPB

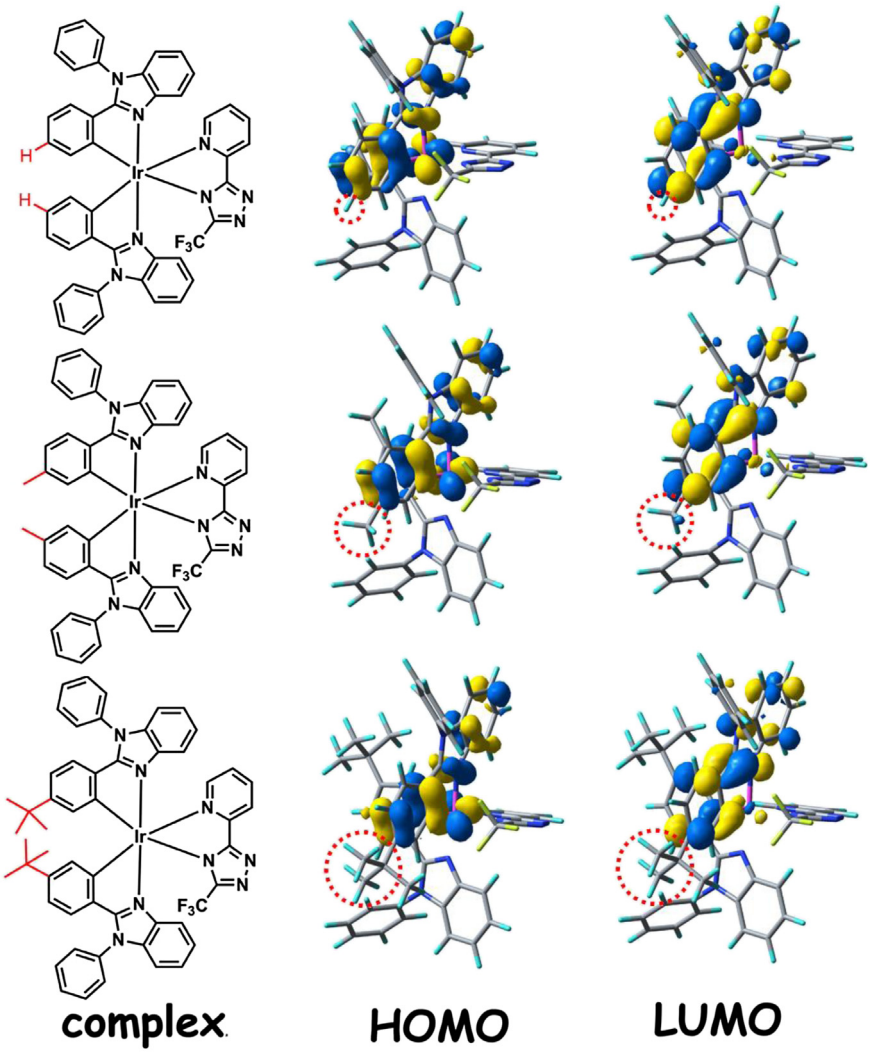

Fig. 2. Electron density distributions of the HOMOs and LUMOs for **1**–**3**.

Table 2
Calculated energy levels, oscillator strengths, and orbital transition analyses of T_1 states for complexes **1**–**3**.

Complex	State	eV	*f*	Assignment	Character
1	T_1	2.22	0.00	H→L (88%)	^{3}MLCT/^{3}LC
2	T_1	2.22	0.00	H→L (89%)	^{3}MLCT/^{3}LC
3	T_1	2.22	0.00	H→L (88%)	^{3}MLCT/^{3}LC

(40 nm)/LiF (0.5 nm)/Mg:Ag (120 nm, 15:1), in which 1,1-bis[4-[*N*,*N*′-di(*p*-tolyl)amino]phenyl]cyclohexane (TAPC) is served as the hole injection layer, 4,4′,4″-tris-(*N*-carbazolyl)-triphenylamine (TCTA) as the hole transporting layer, 1,3,5-tri[(3-pyridyl)-phen-3-yl]benzene (TmPyPB) as the electron transporting layer and LiF as the electron injection layer. The EL intensity versus wavelength curves, the current density–voltage–luminance characteristics and the curves of current efficiency–luminance–power efficiency are presented in Fig. 3. The corresponding EL data are summarized in Table 3.

As shown in Fig. 3(b), the devices **N1**–**N3** reveal the nearly identical emission spectra features with the strong green EL emission peaks at 530–540 nm, which are accompanied by Commission Internationale de L'Eclairage (CIE) coordinates of (0.36, 0.57), (0.38, 0.55) and (0.34, 0.57), respectively. Compared to the devices **N1** and **N2**, the EL spectrum of the device **N3** exhibits a noticeable shoulder peak around 500 nm. Complex **3**-based doped device **C** also exhibits similar EL peak at 500 nm (*vide infra*). In doped devices, the phosphors show the weak intermolecular interactions between the adjacent phosphors due to the introduced host materials. It is thus speculated that incorporation of the *tert*-butyl groups into the cyclometalated ligand is an effective way to reduce the intermolecular interaction, leading to a noticeable shoulder peak around 500 nm for device **N3**. While, non-doped devices **N1** and **N2** showing relatively broad EL spectra should be caused by the strong interactions for complexes **1** and **2** in emitting layer. In addition, the interaction between the emissive layer and the adjacent transporting layers can also widen the emission spectra. The devices **N1** and **N2** exhibit maximum luminances (L_{max}) of 8728 and 7883 cd m^{-2}, maximum current efficiencies of 13.8 and 13.7 cd A^{-1}, maximum power efficiencies of 10.3 and 10.7 lm W^{-1}, respectively. The current and power efficiencies have been significantly improved for device **N3**. It is obvious that the EL efficiencies obtained in device **N3** is the highest among all the devices with $\eta_{c,\,max}$ of 18.6 cd A^{-1}, $\eta_{p,\,max}$ of 16.2 lm W^{-1}. Even at a high brightness of 1000 cd m^{-2}, current efficiency (η_c) is still as high as 16.9 cd A^{-1} and power efficiency (η_p) of 12.6 lm W^{-1}. The low efficiency roll-off is observed for the device **N3**, attributing to the sufficiently reducing intermolecular interaction by the introduction of *tert*-butyl into the cyclometalated ligands of complex **3**. The emission efficiency reported here is significantly higher than that of non-doped device based on Ir(ppy)$_3$ (Fig. S5 in the ESI). The EL performances of **N3** are comparable with some reported iridium(III)-based non-doped devices fabricated using solution process and vapor deposition methods [52,54,74,75]. To investigate the effect of the thickness on the EL performances of the non-doped devices, another three devices, namely **N1-10**, **N2-10**, and **N3-10**, have been fabricated, in which the thickness of the emissive layers are 10 nm. The relevant data is tabulated in Table S2 (ESI). The devices **N1-10**, **N2-10**, and **N3-10** also display decent EL performance with η_c of 18.9, 20.2, and 23.7 cd A^{-1}, η_p of 17.0, 18.1, and 29.2 lm W^{-1}, respectively.

In general, the device with complex **2** as emitter exhibits relatively poor EL performance probably as the intermolecular interaction is reduced a little by incorporating methyl on the PBI. While, *tert*-butyl group is introduced into the PBI of complex **3** to enhance the steric hindrance efficiently, depressing the intermolecular interaction sufficiently. Therefore, the device **N3** exhibits higher EL efficiencies and lower efficiency roll-off. It is a simple and feasible approach to construct efficient iridium(III) complexes suitable for non-doped phosphorescent OLEDs.

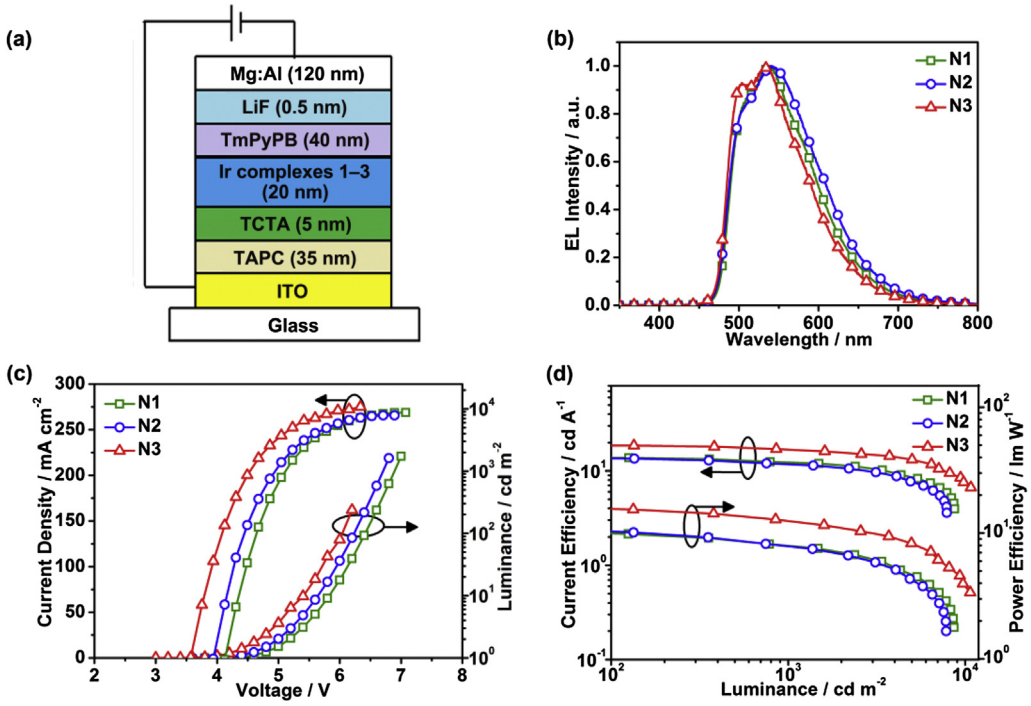

Fig. 3. (a) The general structure and (b) EL spectra of OLEDs **N1**, **N2**, and **N3**. (c) Current density-voltage-luminance and (d) current efficiency-luminance-power efficiency characteristics for OLEDs **N1**–**N3**.

Table 3
Summary of electroluminescence performances for OLEDs.

Device	$V_{turn\text{-}on}$[a] (V)	L_{max}[b] (cd m^{-2}, V)	η_c[b] (cd A^{-1})	η_p[c] (lm W^{-1})	λ_{EL} (nm)	CIE[(x,y), V]
N1	3.8	8728, 7.0	13.8, 12.3	10.3, 8.0	537	(0.36, 0.57), 6.5
N2	3.6	7883, 6.8	13.7, 11.8	10.7, 7.9	540	(0.38, 0.55), 6.5
N3	3.2	10770, 6.2	18.6, 16.9	16.2, 12.6 6	533	(0.34, 0.57), 6.5
A	2.7	11000, 6.8	28.3, 21.9	33.4, 17.0	494	(0.31, 0.54), 7.0
B	2.8	10570, 7.2	24.2, 21.6	21.1, 16.8	495	(0.31, 0.54), 7.0
C	2.6	12640, 6.6	32.9, 24.2	39.6, 19.3	495	(0.30, 0.54), 7.0

[a] Defined as the bias at a brightness of 1 cd m^{-2}.
[b] Maximum power efficiency, then the values at 1000 cd m^{-2}.
[c] Maximum current efficiency, then the values at 1000 cd m^{-2}.

3.3.2. Doped green eletrophosphorecense

To further understand the effect of the substituents on the performance of doped devices, the OLEDs that use them as the dopants have been fabricated. The devices were fabricated under the identical conditions and consisted of ITO/TAPC (30 nm)/TCTA (5 nm)/POAPF:Ir complexes **1**–**3** (10%, 30 nm)/TmPyPB (35 nm)/LiF (0.5 nm)/Mg:Ag (120 nm, 15:1). Because of the great carrier transport abilities and well matched triplet energy gaps (Fig. S4), POAPF is selected as the optimized triplet host for complexes **1**–**3**. Each of the complexes was thus blended into the 2,7-bis(diphenylphosphoryl)-9-(4-diphenylamino)phenyl-9′-phenyl-fluorene (POAPF) as the emitter, with the ratio of POAPF (90 wt%):Ir complexes **1**–**3** (10 wt%). The EL spectra, the current density–voltage–luminance characteristics and the efficiency curves are presented in Fig. 4. The main EL data have been collected in Table 3.

There are no additional emission peaks from POAPF in these devices, indicating an effective energy transfer from the host to dopant. It is observed that the device **C** with complex **3** as emitter exhibits the best EL efficiencies among all the doped devices. The device **C** exhibits excellent EL performance with $\eta_{c,\ max}$ of 32.9 cd A^{-1} and $\eta_{p,\ max}$ of 39.6 lm W^{-1}, however, the η_c and η_p are 24.2 cd A^{-1} and 19.3 lm W^{-1} at the luminance reaches 1000 cd m^{-2}, indicating its significant efficiency decrease in the doped device. Compared with the non-doped EL devices using complexes **1**–**3** as emitting layers, the doped devices exhibit the lower driving voltages. It is likely due to the facilitation of hole and electron injection when POAPF was employed as the host material. In addition, we found that the doped devices show red-shifted EL spectra compared with those of the non-doped ones, which should be caused by the strong intermolecular interactions of the phosphors in the non-doped devices. This is further supported by the obtained EL data for the non-doped devices **N1-10**, **N2-10** and **N3-10**, which exhibit slight bathochromic shifts in EL spectra. For the practical applications, the EL devices showing the low efficiency roll-off are highly desired. As shown in Table 2, we believe that the introduction of *tert*-butyl units into ligands is an efficient way to construction of non-doped phosphors accompanied by low efficiency roll-off values, but may be not suitable for phosphorescent dopants enjoying little efficiency roll-off feature.

4. Conclusions

In summary, we have demonstrated a design strategy of efficient iridium(III) complexes by incorporating different size of substituent

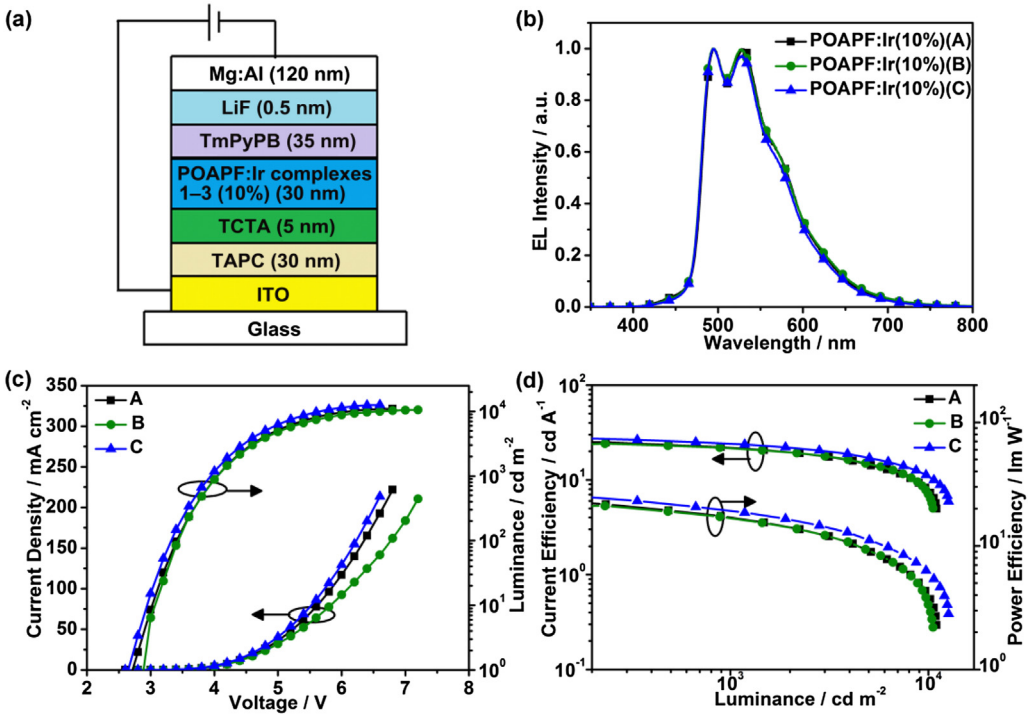

Fig. 4. (a) The general structure and (b) EL spectra of OLEDs **A**, **B**, and **C**. (c) Current density-voltage-luminance and (d) current efficiency-luminance-power efficiency characteristics for OLEDs **A**–**C**.

into the PBI ligand. Three green phosphorescent iridium(III) complexes **1**, **2**, and **3** were synthesized and characterized with the PLQYs of 12.4%, 8.4%, and 15.3% in the neat films, respectively. The PLQY of the complex **3** improves with little affect on the nature of the emitting triplet state and its maximum emission wavelength. Furthermore, with this new phosphors design, the non-doped device based on complex **3** exhibits the L_{max}, $\eta_{c,\ max}$, and $\eta_{p,\ max}$ of 10770 cd m^{-2}, 18.6 cd A^{-1}, and 16.2 lm W^{-1}, respectively, which is higher than those of parent complexes **1** and **2**. The great improvements of EL efficiencies could be attributed to reducing intermolecular interaction in solid state by introduction of bulky substituents on the cyclometalated ligand. Even at a high brightness of 1000 cd m^{-2}, its η_c is still as high as 16.9 cd A^{-1} and η_p of 12.6 lm W^{-1}, exhibiting the low efficiency roll-off. Given the simple molecular structure of iridium(III) complex, the high EL efficiency and low efficiency roll-off for non-doped device, our research provides a simple and promising strategy to develop highly efficient phosphors suitable for non-doped OLEDs.

Acknowledgments

The authors gratefully acknowledge the financial support from National Natural Science Foundation of China (21303012, 21273030, 51203017, 21131001 and 60937001), 973 Program(2013CB834801), China Postdoctoral Science Foundation funded project (2013M540239 and 2014T70269) and the Science and Technology Development Planning of Jilin Province (20130522167JH and 20130204025GX).

Appendix A. Supplementary data

Supplementary data related to this article can be found at http://dx.doi.org/10.1016/j.orgel.2016.05.002.

References

[1] B.W. D'Andrade, S.R. Forrest, White organic light-emitting devices for solid-state lighting, Adv. Mater. 16 (2004) 1585.
[2] L. Duan, J. Qiao, Y. Sun, Y. Qiu, Strategies to design bipolar small molecules for OLEDs: donor-acceptor structure and non-donor-acceptor structure, Adv. Mater. 23 (2011) 1137.
[3] T.-H. Han, Y. Lee, M.-R. Choi, S.-H. Woo, S.-H. Bae, B.H. Hong, J.-H. Ahn, T.-W. Lee, Extremely efficient flexible organic light-emitting diodes with modified graphene anode, Nat. Photonics 6 (2012) 105.
[4] W.C. Choy, W.K. Chan, Y. Yuan, Recent advances in transition metal complexes and light-management engineering in organic optoelectronic devices, Adv. Mater. 26 (2014) 5368.
[5] K.S. Yook, J.Y. Lee, Small molecule host materials for solution processed phosphorescent organic light-emitting diodes, Adv. Mater. 26 (2014) 4218.
[6] Y. Chi, P.T. Chou, Transition-metal phosphors with cyclometalating ligands: fundamentals and applications, Chem. Soc. Rev. 39 (2010) 638.
[7] C. Ulbricht, B. Beyer, C. Friebe, A. Winter, U.S. Schubert, Recent developments in the application of phosphorescent iridium(III) complex systems, Adv. Mater. 21 (2009) 4418.
[8] M.A. Baldo, D.F. O'Brien, Y. You, A. Shoustikov, S. Sibley, M.E. Thompson, S.R. Forrest, Highly efficient phosphorescent emission from organic electroluminescent devices, Nature 395 (1998) 151.
[9] M.A. Baldo, M.E. Thompson, S.R. Forrest, High-efficiency fluorescent organic light-emitting devices using a phosphorescent sensitizer, Nature 403 (2000) 750.
[10] L. Xiao, Z. Chen, B. Qu, J. Luo, S. Kong, Q. Gong, J. Kido, Recent progresses on materials for electrophosphorescent organic light-emitting devices, Adv. Mater. 23 (2011) 926.
[11] W.-Y. Wong, C.-L. Ho, Functional metallophosphors for effective charge carrier injection/transport: new robust OLED materials with emerging applications, J. Mater. Chem. 19 (2009) 4457.
[12] X. Yang, G. Zhou, W.Y. Wong, Functionalization of phosphorescent emitters and their host materials by main-group elements for phosphorescent organic light-emitting devices, Chem. Soc. Rev. 44 (2015) 8484.
[13] W.-Y. Wong, C.-L. Ho, Heavy metal organometallic electrophosphors derived from multi-component chromophores, Coord. Chem. Rev. 253 (2009) 1709.
[14] G. Zhou, W.-Y. Wong, S. Suo, Recent progress and current challenges in phosphorescent white organic light-emitting diodes (WOLEDs), J. Photochem. Photobio. C. Photochem. Rev. 11 (2010) 133.
[15] G. Zhou, W.Y. Wong, X. Yang, New design tactics in OLEDs using functionalized 2-phenylpyridine-type cyclometalates of iridium(III) and platinum(II), Chem. Asian J. 6 (2011) 1706.
[16] L. Ying, C.L. Ho, H. Wu, Y. Cao, W.Y. Wong, White polymer light-emitting devices for solid-state lighting: materials, devices, and recent progress, Adv. Mater. 26 (2014) 2459.
[17] X. Yang, G. Zhou, W.-Y. Wong, Recent design tactics for high performance white polymer light-emitting diodes, J. Mater. Chem. C 2 (2014) 1760.
[18] C.-L. Ho, H. Li, W.-Y. Wong, Red to near-infrared organometallic phosphorescent dyes for OLED applications, J. Organomet. Chem. 751 (2014) 261.
[19] C.-L. Ho, W.-Y. Wong, Small-molecular blue phosphorescent dyes for organic light-emitting devices, New J. Chem. 37 (2013) 1665.
[20] X. Xu, X. Yang, J. Zhao, G. Zhou, W.-Y. Wong, Recent advances in solution-processable dendrimers for highly efficient phosphorescent organic light-emitting diodes (PHOLEDs), Asian J. Org. Chem. 4 (2015) 394.
[21] X. Wang, S.-L. Gong, D. Song, Z.-H. Lu, S. Wang, Highly efficient and robust blue phosphorescent Pt(II) compounds with a phenyl-1,2,3-triazolyl and a pyridyl-1,2,4-triazolyl chelate core, Adv. Funct. Mater. 24 (2014) 7257.
[22] Q. Wang, I.W. Oswald, X. Yang, G. Zhou, H. Jia, Q. Qiao, Y. Chen, J. Hoshikawa-Halbert, B.E. Gnade, A non-doped phosphorescent organic light-emitting device with above 31% external quantum efficiency, Adv. Mater. 26 (2014) 8107.
[23] G. Zhou, Q. Wang, C.-L. Ho, W.-Y. Wong, D. Ma, L. Wang, Duplicating "sunlight" from simple WOLEDs for lighting applications, Chem. Commun. 24 (2009) 3574.
[24] G.-J. Zhou, X.-Z. Wang, W.-Y. Wong, X.-M. Yu, H.-S. Kwok, Z. Lin, New platinum(II) complexes as triplet emitters for high-efficiency monochromatic pure orange electroluminescent devices, J. Organomet. Chem. 692 (2007) 3461.
[25] G. Zhou, Q. Wang, X. Wang, C.-L. Ho, W.-Y. Wong, D. Ma, L. Wang, Z. Lin, Metallophosphors of platinum with distinct main-group elements: a versatile approach towards color tuning and white-light emission with superior efficiency/color quality/brightness trade-offs, J. Mater. Chem. 20 (2010) 7472.
[26] G.-J. Zhou, W.-Y. Wong, B. Yao, Z. Xie, L. Wang, Multifunctional metallophosphors with anti-triplet-triplet annihilation properties for solution-processable electroluminescent devices, J. Mater. Chem. 18 (2008) 1799.
[27] Z. He, W.Y. Wong, X. Yu, H.S. Kwok, Z. Lin, Phosphorescent platinum(II) complexes derived from multifunctional chromophores: synthesis, structures, photophysics, and electroluminescence, Inorg. Chem. 45 (2006) 10922.
[28] W.-Y. Wong, Z. He, S.-K. So, K.-L. Tong, Z. Lin, A multifunctional platinum-based triplet emitter for OLED applications, Organometallics 24 (2005) 4079.
[29] J. Zhang, F. Zhao, X. Zhu, W.-K. Wong, D. Ma, W.-Y. Wong, New phosphorescent platinum(ii) Schiff base complexes for PHOLED applications, J. Mater. Chem. 22 (2012) 16448.
[30] Y.L. Tung, L.S. Chen, Y. Chi, P.T. Chou, Y.M. Cheng, E.Y. Li, G.H. Lee, C.F. Shu, F.I. Wu, A.J. Carty, Orange and red organic light-emitting devices employing neutral Ru(II) emitters: rational design and prospects for color tuning, Adv. Funct. Mater. 16 (2006) 1615.
[31] T.-C. Lee, J.-Y. Hung, Y. Chi, Y.-M. Cheng, G.-H. Lee, P.-T. Chou, C.-C. Chen, C.-H. Chang, C.-C. Wu, Rational design of charge-neutral, near-infrared-emitting osmium(II) complexes and OLED fabrication, Adv. Funct. Mater. 19 (2009) 2639.
[32] O. Bräm, F. Messina, E. Baranoff, A. Cannizzo, M.K. Nazeeruddin, M. Chergui, Ultrafast relaxation dynamics of osmium–polypyridine complexes in solution, J. Phys. Chem. C 117 (2013) 15958.
[33] Y. Chi, B. Tong, P.-T. Chou, Metal complexes with pyridyl azolates: design, preparation and applications, Coord. Chem. Rev. 281 (2014) 1.
[34] K. Udagawa, H. Sasabe, C. Cai, J. Kido, Low-driving-voltage blue phosphorescent organic light-emitting devices with external quantum efficiency of 30%, Adv. Mater. 26 (2014) 5062.
[35] J. Lee, H.F. Chen, T. Batagoda, C. Coburn, P.I. Djurovich, M.E. Thompson, S.R. Forrest, Deep blue phosphorescent organic light-emitting diodes with very high brightness and efficiency, Nat. Mater. 15 (2015) 92.
[36] Y. You, W. Nam, Photofunctional triplet excited states of cyclometalated Ir(III) complexes: beyond electroluminescence, Chem. Soc. Rev. 41 (2012) 7061.
[37] E. Holder, B.M.W. Langeveld, U.S. Schubert, New trends in the use of transition metal-ligand complexes for applications in electroluminescent devices, Adv. Mater. 17 (2005) 1109.
[38] W.Y. Wong, C.L. Ho, Z.Q. Gao, B.X. Mi, C.H. Chen, K.W. Cheah, Z. Lin, Multifunctional iridium complexes based on carbazole modules as highly efficient electrophosphores, Angew. Chem. Int. Ed. 45 (2006) 7800.
[39] S. Gong, Q. Fu, Q. Wang, C. Yang, C. Zhong, J. Qin, D. Ma, Highly efficient deep-blue electrophosphorescence enabled by solution-processed bipolar tetraarylsilane host with both a high triplet energy and a high-lying HOMO level, Adv. Mater. 23 (2011) 4956.
[40] L. Deng, T. Zhang, R. Wang, J. Li, Diphenylphosphorylpyridine-functionalized iridium complexes for high-efficiency monochromic and white organic light-emitting diodes, J. Mater. Chem. 22 (2012) 15910.
[41] B. Zhang, G. Tan, C.S. Lam, B. Yao, C.L. Ho, L. Liu, Z. Xie, W.Y. Wong, J. Ding, L. Wang, High-efficiency single emissive layer white organic light-emitting diodes based on solution-processed dendritic host and new orange-emitting iridium complex, Adv. Mater. 24 (2012) 1873.
[42] J. Kalinowski, W. Stampor, J. Mężyk, M. Cocchi, D. Virgili, V. Fattori, P. Di Marco, Quenching effects in organic electrophosphorescence, Phys. Rev. B 66 (2002) 126.
[43] T. Peng, Y. Yang, H. Bi, Y. Liu, Z. Hou, Y. Wang, Highly efficient white organic electroluminescence device based on a phosphorescent orange material

doped in a blue host emitter, J. Mater. Chem. 21 (2011) 3551.
[44] G. Zhou, W.Y. Wong, B. Yao, Z. Xie, L. Wang, Triphenylamine-dendronized pure red iridium phosphors with superior OLED efficiency/color purity trade-offs, Angew. Chem. Int. Ed. 46 (2007) 1149.
[45] H. Wu, G. Zhou, J. Zou, C.-L. Ho, W.-Y. Wong, W. Yang, J. Peng, Y. Cao, Efficient polymer white-light-emitting devices for solid-state lighting, Adv. Mater. 21 (2009) 4181.
[46] J. Zou, H. Wu, C.S. Lam, C. Wang, J. Zhu, C. Zhong, S. Hu, C.L. Ho, G.J. Zhou, H. Wu, W.C. Choy, J. Peng, Y. Cao, W.Y. Wong, Simultaneous optimization of charge-carrier balance and luminous efficacy in highly efficient white polymer light-emitting devices, Adv. Mater. 23 (2011) 2976.
[47] G. Zhou, C.-L. Ho, W.-Y. Wong, Q. Wang, D. Ma, L. Wang, Z. Lin, T.B. Marder, A. Beeby, Manipulating charge-transfer character with electron-withdrawing main-group moieties for the color tuning of iridium electrophosphors, Adv. Funct. Mater. 18 (2008) 499.
[48] S. Chen, G. Tan, W.-Y. Wong, H.-S. Kwok, White organic light-emitting diodes with evenly separated red, green, and blue colors for efficiency/color-rendition trade-off optimization, Adv. Funct. Mater. 21 (2011) 3785.
[49] X. Xu, X. Yang, J. Dang, G. Zhou, Y. Wu, H. Li, W.-Y. Wong, Trifunctional IrIII ppy-type asymmetric phosphorescent emitters with ambipolar features for highly efficient electroluminescent devices, Chem. Commun. 50 (2014) 2473.
[50] C.L. Ho, W.Y. Wong, Z.Q. Gao, C.H. Chen, K.W. Cheah, B. Yao, Z.Y. Xie, Q. Wang, D.G. Ma, L.X. Wang, X.M. Yu, H.S. Kwok, Z.Y. Lin, Red-light-emitting iridium complexes with hole-transporting 9-arylcarbazole moieties for electrophosphorescence efficiency/color purity trade-off optimization, Adv. Funct. Mater. 18 (2008) 319.
[51] H.A. Al Attar, A.P. Monkman, Dopant effect on the charge injection, transport, and device efficiency of an electrophosphorescent polymeric light-emitting device, Adv. Funct. Mater. 16 (2006) 2231.
[52] Y. Wang, N. Herron, V.V. Grushin, D. LeCloux, V. Petrov, Highly efficient electroluminescent materials based on fluorinated organometallic iridium compounds, Appl. Phys. Lett. 79 (2001) 449.
[53] Y.H. Song, S.J. Yeh, C.T. Chen, Y. Chi, C.S. Liu, J.K. Yu, Y.H. Hu, P.T. Chou, S.M. Peng, G.H. Lee, Bright and efficient, non-doped, phosphorescent organic red-light-emitting diodes, Adv. Funct. Mater. 14 (2004) 1221.
[54] L. Chen, Z. Ma, J. Ding, L. Wang, X. Jing, F. Wang, Self-host heteroleptic green iridium dendrimers: achieving efficient non-doped device performance based on a simple molecular structure, Chem. Commun. 47 (2011) 9519.
[55] W. Tian, C. Yi, B. Song, Q. Qi, W. Jiang, Y. Zheng, Z. Qi, Y. Sun, Self-host homoleptic green iridium dendrimers based on diphenylamine dendrons for highly efficient single-layer PhOLEDs, J. Mater. Chem. C 2 (2014) 1104.
[56] M.R. Zhu, Y.H. Li, J.S. Miao, B. Jiang, C.L. Yang, H. Wu, J.G. Qin, Y. Cao, Multifunctional homoleptic iridium(III) dendrimers towards solution-processed nondoped electrophosphorescence with low efficiency roll-off, Org. Electron 15 (2014) 1598.
[57] J. Ding, J. Lü, Y. Cheng, Z. Xie, L. Wang, X. Jing, F. Wang, Solution-processible red iridium dendrimers based on oligocarbazole host dendrons: synthesis, properties, and their applications in organic light-emitting diodes, Adv. Funct. Mater. 18 (2008) 2754.
[58] L. Chen, J. Ding, Y. Cheng, Z. Xie, L. Wang, X. Jing, F. Wang, Bipolar heteroleptic green iridium dendrimers containing oligocarbazole and oxadiazole dendrons for bright and efficient nondoped electrophosphorescent devices, Chem. Asian J. 6 (2011) 1372.
[59] M. Zhu, J. Zou, X. He, C. Yang, H. Wu, C. Zhong, J. Qin, Y. Cao, Triphenylamine dendronized iridium(III) complexes: robust synthesis, highly efficient nondoped orange electrophosphorescence and the structure–property relationship, Chem. Mater. 24 (2012) 174.
[60] H.-T. Cao, G.-G. Shan, Y.-M. Yin, H.-Z. Sun, Y. Wu, W.-F. Xie, Z.-M. Su, Modification of iridium(III) complexes for fabrication of high-performance non-doped organic light-emitting diode, Dyes Pigm. 112 (2015) 8.
[61] H. Cao, G. Shan, X. Wen, H. Sun, Z. Su, R. Zhong, W. Xie, P. Li, D. Zhu, An orange iridium(iii) complex with wide-bandwidth in electroluminescence for fabrication of high-quality white organic light-emitting diodes, J. Mater. Chem. C 1 (2013) 7371.
[62] X. Huixia, S. Peng, Z. Dan, Y. Tingting, H. Yuying, W. Hua, S. Heping, X. Bingshe, Synthesis and photoelectric performances of blue-green emitting iridium phenylpyridine complexes using N,N′-heteroaromatic ancillary ligands, New J. Chem. 39 (2015) 5293.
[63] J. Sun, H. Wang, H. Xu, J. Li, Y. Wu, X. Du, B. Xu, Synthesis, structure, photophysical and electroluminescent properties of a blue-green self-host phosphorescent iridium(III) complex, Mater. Chem. Phys. 162 (2015) 392.
[64] X. Huixia, Y. Yan, Q. Litao, H. Yuying, W. Hua, C. Liuqing, X. Bingshe, Synthesis and characterization of blue-to-green electrophosphorescence emitter based on pyrazole iridium complexes, Dyes Pigm. 99 (2013) 67.
[65] A.D. Becke, Density-functional thermochemistry. III. The role of exact exchange, J. Chem. Phys. 98 (1993) 5648.
[66] G.M. Sheldrick, SHELXL-97, Program for Crystal Structure Refinement, University of Gottingen, 1997.
[67] M.K. Nazeeruddin, R. Humphry-Baker, D. Berner, S. Rivier, L. Zuppiroli, M. Graetzel, Highly phosphorescence iridium complexes and their application in organic light-emitting devices, J. Am. Chem. Soc. 125 (2003) 8790.
[68] Q.-L. Xu, X. Liang, S. Zhang, Y.-M. Jing, X. Liu, G.-Z. Lu, Y.-X. Zheng, J.-L. Zuo, Efficient OLEDs with low efficiency roll-off using iridium complexes possessing good electron mobility, J. Mater. Chem. C 3 (2015) 3694.
[69] L. He, L. Duan, J. Qiao, R. Wang, P. Wei, L. Wang, Y. Qiu, Blue-emitting cationic iridium complexes with 2-(1H-Pyrazol-1-yl)pyridine as the ancillary ligand for efficient light-emitting electrochemical cells, Adv. Funct. Mater. 18 (2008) 2123.
[70] H.T. Cao, G.G. Shan, Y.M. Yin, H.Z. Sun, Y. Wu, W.F. Xie, Z.M. Su, Manipulating efficiencies through modification of N-heterocyclic phenyltriazole ligands for blue iridium(III) complexes, Dyes Pigm. 113 (2015) 655.
[71] J. Ding, B. Wang, Z. Yue, B. Yao, Z. Xie, Y. Cheng, L. Wang, X. Jing, F. Wang, Bifunctional green iridium dendrimers with a “self-host” feature for highly efficient nondoped electrophosphorescent devices, Angew. Chem. Int. Ed. 48 (2009) 6664.
[72] B. Tong, H.-Y. Ku, I.J. Chen, Y. Chi, H.-C. Kao, C.-C. Yeh, C.-H. Chang, S.-H. Liu, G.-H. Lee, P.-T. Chou, Heteroleptic Ir(iii) phosphors with bis-tridentate chelating architecture for high efficiency OLEDs, J. Mater. Chem. C 3 (2015) 3460.
[73] D. Chen, L. Han, D. Liu, K. Ye, Y. Liu, J. Zhang, Y. Wang, High performance blue-green and green phosphorescent OLEDs based on iridium complexes with N^C^N-coordinated terdentate ligands, RSC Adv. 5 (2015) 18328.
[74] Z. Liu, Z. Bian, L. Ming, F. Ding, H. Shen, D. Nie, C. Huang, Green and blue-green phosphorescent heteroleptic iridium complexes containing carbazole-functionalized β-diketonate for non-doped organic light-emitting diodes, Org. Electron 9 (2008) 171.
[75] W. Tian, Q. Qi, B. Song, C. Yi, W. Jiang, X. Cui, W. Shen, B. Huang, Y. Sun, A bipolar homoleptic iridium dendrimer composed of diphenylphosphoryl and diphenylamine dendrons for highly efficient non-doped single-layer green PhOLEDs, J. Mater. Chem. C 3 (2015) 981.